Am. J. Hum. Genet. 59:308–319, 1996

Exhaustive Mutation Scanning by Fluorescence-Assisted Mismatch Analysis Discloses New Genotype-Phenotype Correlations in Angioedema

Elisabeth Verpy,[1] Michel Biasotto,[1,*] Melchiorre Brai,[2] Gabriella Misiano,[2] Tommaso Meo,[1] and Mario Tosi[1]

[1]Unité d'Immunogénétique et INSERM U 276, Institut Pasteur, Paris; and [2]Istituto di Patologia Generale, Palermo

Summary

A complete mutational scan of the gene coding for the serpin C1 inhibitor, comprising all eight exons and adjacent intron sequences and 550 bp preceding the transcription start site, was rapidly accomplished in 36 unrelated angioedema patients by using fluorescence-assisted mismatch analysis (FAMA). Mutations accounting for C1 inhibitor deficiency were identified in every one of 34 patients, with two failures turning out to be spurious cases. Two new substitution dimorphisms were also detected in introns. Changes affecting the C1 inhibitor protein, distributed throughout the seven coding exons, provide new insights into the molecular pathology of serpins. Six different splice-site and two promoter mutations were also found. Among the latter, a C→T transition within one of two putative CAAT boxes of this TATA-less promoter, the sole idiomorphic nucleotide change in this kindred, was found homozygous in the proband, at variance with the dominant mode of transmission observed for structural mutations. FAMA, in the chemical probes configuration used in this study, is a rapid and robust mutation-scanning procedure, applicable to large DNA segments or transcripts and proved capable of 100% detection. Moreover, it provides accurate positional information—and hence recognition of multiple substitutions, precise relationship with those already known, and often immediate identification of the nucleotide change.

Introduction

The ongoing discovery of genes either directly responsible for inherited diseases or contributing to pathological conditions underscores the need for efficient methods of detection of unknown mutations. In spite of constant improvements of the sequencing chemistries and attendant softwares for heterozygote detection, direct automated sequencing of PCR products does not guarantee complete mutation detection and requires time-consuming and costly optimizations (Kwok et al. 1994; Phelps et al. 1995), not yet suited to diagnostic tasks (Phelps et al. 1995). Among DNA-scanning methods, those based on cleavage of heteroduplex DNA at mispaired or unpaired bases and sizing of the truncated DNA strands have proved effective in the screening of large DNA regions (for a review, see Grompe 1993). Detection and sizing of cleavage products recently has been potentiated by the introduction of multiple fluorescent labels, used to increase throughput (Haris et al. 1994; Rowley et al. 1995) or to maximize diagnostic accuracy (i.e., lack of false-negatives), sensitivity on dilution of the mutant sequence, and positional precision (Verpy et al. 1994).

In the present study we have sought to validate the power of bichrome fluorescent labeling (Verpy et al. 1994), by searching the mutations in the *C1 INH* gene (Stoppa-Lyonnet et al. 1987; Carter et al. 1991), which are responsible for hereditary angioedema (HAE), a dominantly transmitted disease characterized by acute, often serious, subcutaneous or mucosal swellings, due to C1 inhibitor (C1 inh) deficiency. This serpin is the only plasma inhibitor of the enzymic activity of the first component of complement, but it also plays a major role in the control of kallikrein and coagulation factor XII activities (for a review see Davis 1988). According to the plasma level of C1 inh, two types of HAE traditionally have been recognized: the more common form (type I), with protein levels in the 5%–30% range of normals, and the less frequent form (type II), characterized by normal or even high antigenic levels and low functional activity (Rosen et al. 1965). Most type II patients (Davis et al. 1992 and references therein) have single amino acid substitutions at the reactive-center residue or in a region located on the N-terminal side of the reactive-center loop, which is called the "proximal hinge" region (Stein and Carrell 1995; Perry and Carrell

Received March 8, 1996; accepted for publication May 28, 1996.

Address for correspondence and reprints: Dr. Mario Tosi, Unité d'Immunogénétique et INSERM U 276, Institut Pasteur, 25 rue du Docteur Roux, 75724 Paris Cedex 15, France.

*Deceased, July 17, 1995.

0002-9297/96/5902-0006$02.00

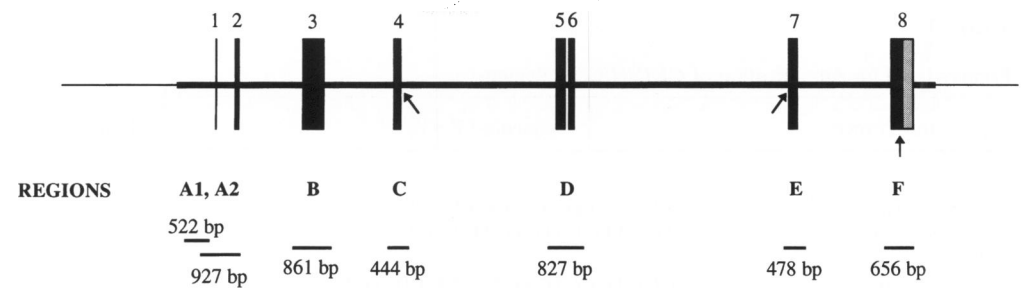

Figure 1 Screening strategy. Shown are the *C1 INH* gene structure and regions scanned. Exons are represented by boxes. The 3′ UTR is shaded. PCR-amplified regions are represented by thick lines and extend across all exon/intron boundaries and up to position −591 from the transcription start site. Arrows point to three polymorphic markers, of which only that in exon 8 (restriction site *Hgi*AI) has been reported elsewhere (Bock et al. 1986).

1996). The latter mutations either block the interaction with the target proteases or convert the inhibitor into a substrate (Davis et al. 1992). Here, we demonstrate the advantages that accrue from exhaustive detection of mutations in a hereditary disease, especially with regard to previously unrecognized subtypes and to the unexpected recessive expression of a regulatory mutation in a typically dominant disease.

Subjects and Methods

Subjects

We studied 36 unrelated HAE patients who had not shown *C1 INH* gene alterations in a previous DNA-blot analysis (Stoppa-Lyonnet et al. 1991). They had been diagnosed as type I HAE, except for one patient, initially diagnosed as a sporadic type II case. At least nine of these patients were candidates for de novo mutations, because a thorough investigation of their families failed to reveal other occurrences of the disease. Two healthy individuals were also included as controls. Eight different point mutations have been found in these patients in previous screenings limited to exon 8 (Verpy et al. 1994, 1995).

Fluorescence-Assisted Mismatch Analysis (FAMA)

The *C1 INH* gene, which maps to 11q12-q13 (Janson et al. 1991 and references therein), consists of eight exons distributed over a stretch of DNA of ~17 kb and contains 17 *Alu* repeats within introns. *Alu*-mediated partial deletions/duplications account for ~15% of genetic deficiencies of C1 inhibitor (Stoppa-Lyonnet et al. 1991). For each region (see fig. 1), 100–500 ng of genomic DNA isolated from peripheral white blood cells was subjected to 30 or 35 cycles of PCR amplification in a 50-μl reaction using the external oligonucleotide primers indicated in table 1. The fluorescence-labeled templates were generated by reamplifying, typically for 25 cycles, an aliquot of the first amplification reaction, by using internal fluorescent primers (nested PCR) as indicated in table 1, except for region 6, for which the same primers were labeled with appropriate fluorescent dyes. Initially, primers were labeled by coupling a dye N-hydroxyl succinimide ester (FAM and JOE fluorophores [Perkin Elmer, Applied Biosystems Division] for the forward and reverse primer respectively), by using an amino-hexyl linker attached onto the 5′ end, according to the Perkin Elmer/Applied Biosystems protocol. Subsequently, the fluorescent dye phosphoramidites 6-FAM (for the forward primer) and HEX (for the reverse primer) were used to synthesize directly fluorescent dye-labeled oligonucleotides.

The basic protocol for FAMA (Verpy et al. 1994) was followed, with few important modifications (Biasotto et al. 1996). Notably, hydroxylamine and osmium tetroxide working solutions were stored in small aliquots at −80°C for as long as several months, thus ensuring reproducibility and removing potential hazards associated with their repeated preparation. One picomole of bichrome PCR fragments was boiled for 5 min in 150 μl of 0.3 M NaCl/3.5 mM $MgCl_2$/3 mM Tris-HCl, pH 7.7, and annealed at 65°C overnight or ≥5 h. The heteroduplexes were ethanol precipitated after addition of 60 μg of glycogen (Boerhinger-Mannheim) and were resuspended in 18 μl of H_2O. Six microliters of DNA were treated either at 37°C for 45 min with 20 μl of the freshly thawed hydroxylamine working solution or at room temperature for 15 min with 0.4% osmium tetroxide/2% or 2.5% pyridine/0.5 mM Na_2EDTA/5 mM Hepes, pH 8 (final concentrations), in a total volume of 25 μl, by using siliconized tubes. Modification reactions were terminated by transferring the samples to ice and adding 200 μl of cold stop solution (0.3 M sodium acetate/0.1 mM Na_2EDTA, pH 5.2), and the nucleic acids were ethanol precipitated once in a dry-ice ethanol bath, washed in 70% ethanol, resuspended in 50 μl of 1 M piperidine, and incubated at 90°C for 20 min. After the samples were cooled on ice, 50 μl of 0.6 M sodium acetate were added, and the nucleic acids were ethanol

Table 1

Primers Used for Amplification of *C1 INH* Gene Regions

Region and Primer[a]	Sequence (5′→3′)[b]	Position 5′[c]
A:		
ex Forward	TTAGGTTGAATGCTTGTTGA	−614
ex Reverse	TGCATCTGTCTGAGTCCTGA	829
A1:		
in Forward	GGGTGCCTCACATCCGTTGTCT	−591
in Reverse	GGGACACTGCCCAGTTACAAATTA	−70
A2:		
in Forward	GGGCTAAATTCCTGGCCTGGCC	−193
in Reverse	GGAGCCTGAAGGGTTAATCCTCA	734
B:		
ex Forward	CTGACTATCCCTCATCTTC	1951
ex Reverse	TTAGTGGCTGCGACCTTAT	2947
in Forward	aaGTGGTTCTAAGACAGATTGCTCAT	2038
in Reverse	gAAGCAATCGTGCCTATTACATCAC	2895
C:		
ex Forward	GCAGCCTAGTGTCTGACTT	3735
ex Reverse	GCCAGAGACTTGTCTAAGG	4696
in Forward	GAGAGAACATTCCAGCTCAGATGA	4207
in Reverse	GGAGTGACCTAATGCTCCTGCC	4650
D:		
ex Forward	CCATAGTCACATAGCAAGCTGA	8076
ex Reverse	TGAGAATCCTGTTTCCAGCCTA	9075
in Forward	ATCTGTAAGAGGAGTGGGCTGG	8171
in Reverse	GGTGGAAATACAGATGGAAGGAG	8997
E:		
ex Forward	CCAGCACAGAGTTGGATCA	13834
ex Reverse	TGAGCCTCCATTTCCACAAT	14431
in Forward	GGAAGCTTAGGTCTGACTGATGC	13896
in Reverse	AGGGTTGCAGGACAAACTGAGATT	14373
F:		
Forward[d]	tGAGGATCCCACGAACTGCCAG	16474
Reverse[d]	GTGAACTTGAACTAGAGAAAGC	17128

[a] ex = external reaction; and in = internal reaction.
[b] Bases denoted by lowercase letters at the 5′ end of some primers differ from those in the *C1 INH* sequence.
[c] Numbering is that of Carter et al. (1991).
[d] Unlabeled and fluorescence-labeled primers were the same.

precipitated, washed twice in 70% ethanol, and lyophilized. The pellets were resuspended in 8 μl of gel-loading solution containing deionized formamide and 50 mM Na_2EDTA, pH 8.0, in a 5:1 ratio. Two to four microliters of each sample were analyzed on an automated ABI 373A sequencer, as described. Fluorescence signals were routinely analyzed starting at ~70 nucleotides from the fluorophore.

Direct Sequencing of PCR Products

The PCR products were purified by using Ultrafree-MC filter units (Millipore) to remove unincorporated oligonucleotide primers. The fragments were then sequenced according to the ABI protocol for *Taq*-dye terminator cycle sequencing on an automated ABI 373A sequencer.

Results

Screening Strategy

Thirty-six unrelated HAE patients with or without family history were screened for point mutations, according to the strategy described in figure 1. By use of oligonucleotide primers in introns and in the 5′ and 3′ flanking regions of the *C1 INH* gene (table 1), seven bichrome DNA fragments were produced from six different regions by two-step PCR amplification. These amplicons encompass individual exons or groups thereof and cover all intron-exon boundaries as well as a stretch of 591 bp preceding the transcription start site (fig. 1). The fluorescence-labeled 5′ ends of primers were positioned in introns at 100–200 bp from the exon boundary. We first tried to screen region A by using a single

1,325-bp-long amplicon, a size proved successful in FAMA scanning of a large number of amplicons from other genes (authors' unpublished data). However, we were unable to form correct heteroduplexes with this particular amplicon. Even when more stringent hybridization conditions were used, the duplexes formed migrated in nondenaturing PAGE as a smear with mobility lower than that of the corresponding homoduplexes, suggesting formation of internal structures on separation of the DNA strands. This difficulty was overcome by dividing the region into two overlapping PCR fragments.

For each region, mutation scanning was performed simultaneously on serial arrangements of patients, because the ultimate sensitivity of FAMA depends on the information obtained by superimposing electrophoretic profiles of the same region from different individuals (Verpy et al. 1994). Mutations were further characterized by targeted sequencing of the relevant site. When other regions were examined, only patients with mutations leading to premature termination of translation were excluded from subsequent screenings.

Heterozygous Mutations in 33 of 36 Unrelated Angioedema Patients

The foregoing strategy allowed detection of heterozygous mutations in 33 patients. Two previously unknown dimorphisms (see below) were also found, in addition to the known *Hgi*AI polymorphism in exon 8 (Bock et al. 1986). Mutations found in each region are listed in table 2 in the order in which amplicons have been scanned for mutations. Family studies or cloning of the relevant region demonstrated the presence of double mutations in a *cis* configuration in patients 40, 31, and 25 (discussed below). Only three pathogenic changes were found to be shared by two apparently unrelated patients: 16872 C→T in exon 8 (patients 12 and 22), 2694 G→A in exon 3 (patients 20 and 28)—both occurring at CpG dinucleotides—and 2650 T→C in exon 3 (patients 24 and 25).

Microdeletions/Duplications

Eleven small deletions/insertions are shown with underlined characters in table 2. Most of them result in frameshifts (discussed below). However, a 29-bp deletion, found in patient 13, encompasses the intron 6/exon 7 junction (fig. 2). Its boundaries fall within the CTCT sequence, which is conserved on the 3′ side of two almost perfect repeats TGCATCTCT (nucleotides 14012–14020 and 1441–14049; conserved residues are underlined). The same splice site is altered in patient 29, whose last two bases of intron 6 and first two bases of exon 7 are replaced by the GCA triplet (fig. 2). This change generates a new potential acceptor site (fig. 2) and duplicates a CTGCAG *Pst*I recognition site present in the normal sequence 13 nucleotides downstream.

Other Splice-Site Mutations

The acceptor splice site of intron 6 (fig. 2) is also affected by a G→C transversion that changes the canonical AG. Similarly, the invariant G of the acceptor splice site of intron 1 was found to be substituted by A. Different mutations (at positions marked by underlined letters in the consensus sequence AGgt$^{a}/_{g}$agt) were found at the donor splice sites of intron 2 and of intron 3. As also is shown in figure 2, a G is present at the last position of exons and at the fifth position of introns in 81% and 85%, respectively, of the donor sites in primates (Senapathy et al. 1990). The consequences of these splice-site mutations will have to be examined at the mRNA level in peripheral blood monocytes. They may result in quantitative (i.e., reduced amount of a normal mRNA) or qualitative defects, through exon skipping, activation of a cryptic site, or generation of a new splice site, as probably is the case for the agGT→gca substitution at the intron 6/exon 7 junction (fig. 2). Use of this new splice site would lead to deletion of the conserved V322 (codon GTG). In another study, a mutation of the invariant G of the donor splice site of intron 6 of *C1 INH* has been reported (Siddique et al. 1991). In this case no abnormal mRNA was detected, and the normal mRNA was present, with a relative abundance of 50%, suggesting that the transcript of the mutant allele was not converted into a stable mRNA.

Premature Protein Termination

Mutations of the translation-termination type (frameshift or nonsense), found in 12 patients, were distributed over all coding exons (table 2 and fig. 3*A*). In exon 5 of patient 9, deletion of a C within a group of four cytosines (positions 8380–8383) produces a frameshift and causes premature termination at codon 229. The same stop codon results from deletion of C8390 in patient 41. A 2-bp deletion in exon 6 (positions 8814–8815 in patient 17) and a 2-bp deletion in exon 3 (positions 2250–2251 in patient 6) also result in premature termination. The latter deletion occurs within an $(AG)_3$ repeat. Again in exon 3 (in patient 37), an expansion from two to four T residues at position 2677–2678 results in translation of 32 out-of-frame amino acids, followed by protein termination at codon 189, encoded in exon 4. Two frameshift mutations were also found in exon 4—that is, the insertion of an A at position 4372, within a stretch of four consecutive adenines (patient 21), and deletion of a C within a stretch of four cytosines at positions 4397–4400 (patient 16). A tandem duplication of eight nucleotides (589–596) within exon 2 (patient 27) produces a frameshift and results in translation of only three altered

Table 2

Mutations Identified in 34 Patients

Region and Patient[a]	Location	Nucleotide Change[b]	Predicted Effect on Transcript/Protein
F:[c]			
10	Exon 8	16809 G→A	V451M
40[d]	Exon 8	16812 C→G	Q452E
34	Exon 8	16822 T→C	F455S
19	Exon 8	16834 T→C	L459P
40[d]	Exon 8	16834 T→G	L459R
33	Exon 8	16858 C→G	P467R
12	Exon 8	16872 C→T	R472 stop
22	Exon 8	16872 C→T	R472 stop
30	Exon 8	16884 C→T	P476S
D:			
26	Exon 5	8346 T→C	F214S
9	Exon 5	8383 ΔC	P226-X_2-stop[e]
41	Exon 5	8390 ΔC	V228-stop
31[d]	Exon 5	8455–8457 ΔCAA	ΔN250
23	Exon 6	8741 T→G	F281C
11	Exon 6	8807 T→C	M303T
17	Exon 6	8814–8815 ΔCA	N304-X_9-stop
43	Exon 6	8823 C→G	Y308 stop
B:			
6	Exon 3	2250–2251 ΔAG	E13-X_{20}-stop
24	Exon 3	2650 T→C	F147S
25[d]	Exon 3	2650 T→C	F147S
14	Exon 3	2656 C→T	P149L
37	Exon 3	2679 ins TT	L156-X_{32}-stop
20	Exon 3	2694 G→A	Splicing defect or G162R
28	Exon 3	2694 G→A	Splicing defect or G162R
C:			
21	Exon 4	4372 ins A	K168-X_{65}-stop
16	Exon 4	4400 ΔC	P178-X_9-stop
E:			
13	Intron 6-exon 7	14019–14047 Δ29 bp	Splicing defect
29	Intron 6-exon 7	14029 AGGT→GCA	Splicing defect
15	Intron 6	14030 G→C	Splicing defect
35	Exon 7	14037 C→T	Q324stop
18	Exon 7	14181 A→C	T372P
A:			
31[d]	Promoter	−40 C→G	?
36	Intron 1	564 G→A	Splicing defect
25[d]	Exon 2	566 T→C	?
27	Exon 2	589–596 8-bp duplication	R-19-X_3-stop
46	Intron 2	642 G→A	Splicing defect
44	Promoter	−103 C→T[f]	Transcriptional defect?

[a] Mutations occurring independently are underlined.

[b] Numbering is that of Carter et al. (1991). Small deletions or insertions are denoted by underlined characters, and their nature is indicated: Δ = deletion; and ins = insertion.

[c] Mutations in region F were previously found with conventional CCM (Verpy et al. 1995).

[d] Patient had two mutations in *cis*.

[e] Frameshift mutations are denoted by the last correct amino acid followed by the number of misincorporated residues before the stop codon.

[f] Proband is homozygous.

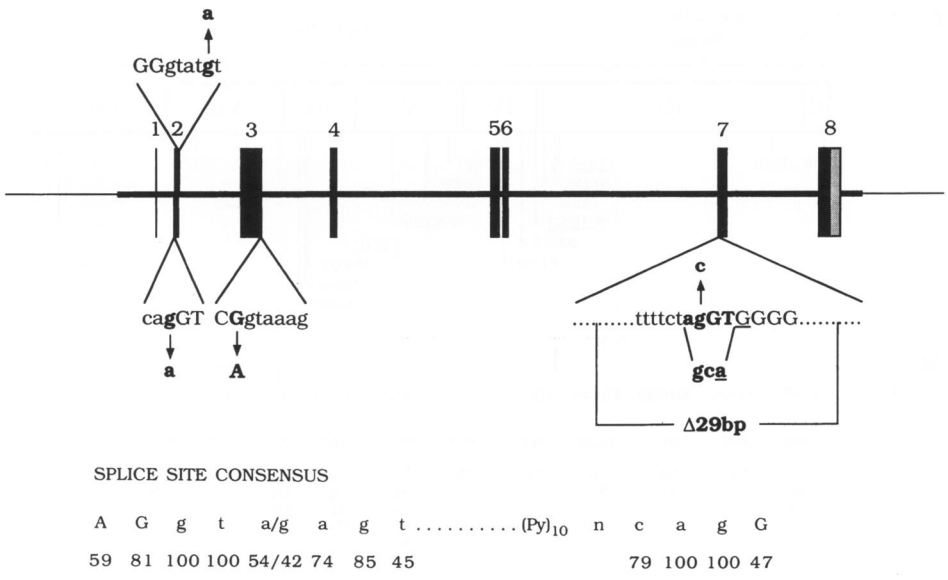

Figure 2 Splice-site mutations. Six different splice-site mutations were found, including a 29-bp deletion and a deletion/substitution. The latter and an independent point mutation affect the intron 6/exon 7 junction. Note that substitution of the agGT quadruplet with the gca triplet generates a new potential acceptor site (underlined aG). The 642 G→A transition at the fifth position of intron 2 (patient 46) is predicted to be pathogenic, on the basis of the consensus sequence of the donor splice sites. Similarly, the 2694 G→A transition at the last base of exon 3 (patients 20 and 28; see table 2) is predicted to result into a splicing defect but may also determine a glycine-to-arginine substitution. Note, however, that only these mutations were found, respectively, in patient 46 and in patients 20 and 28, on complete scanning of the *C1 INH* gene.

amino acids before a stop codon within the signal peptide. This duplication occurs just two nucleotides upstream of a perfect 9-bp direct repeat present in the normal sequence (GCTGACCCT: 598–606, 607–615), suggesting that replication slippage is the most likely mutational mechanism involved. Besides this premature termination in the signal peptide and a nonsense mutation in exon 8 (R472stop), which results in the synthesis of a protein only seven residues shorter than the normal one but rapidly degraded intracellularly (Verpy et al. 1995), all other frameshift or nonsense mutations identified in this study predict the synthesis of protein products lacking the reactive-site loop. Four exon 8 mutations with predicted termination a short distance upstream of the reactive-site loop have already been described elsewhere (Frangi et al. 1991; Siddique et al. 1992, 1993).

Missense Mutations

Fourteen different missense mutations and two deletions of a single codon were found (fig. 3). Among the latter, the ΔV322 mutant protein (first codon of exon 7; shown in parentheses in fig. 3) will be produced only if the new canonical splice site generated by the 14029 agGT→gca substitution is used (see fig. 2). Two additional mutant proteins, also shown in parentheses in figure 3, may not be expressed or may be produced only in low amounts, either because of a concomitant splicing defect (G162R, predicted from the point mutation 2656 G→A at the last base of exon 3) or, in the case of the ΔN250 deletion, because of a potential promoter defect associated in *cis*, as discussed below. All missense mutations affect the serpin domain of C1 inh (see fig. 3*A*), and it is not surprising that no amino acid substitution was found in the N-terminal portion of the protein, characteristically present only in C1 inh and highly O-glycosylated (see fig. 3*A*). Deletion of this domain has indeed little or no effect on C1 inh secretion and in vitro functional activity (Coutinho et al. 1994; authors' unpublished data). At six positions (fig. 3*B*), amino acids affected by missense mutations in C1 inh also have been found substituted or deleted in α1-antitrypsin (Graham et al. 1989; Curiel et al. 1990) or antithrombin III (Lane et al. 1992; Millar 1995) in patients with emphysema or recurrent thromboembolic disease, respectively (reviewed in Stein and Carrell 1995). Among the eight different C1 inh mutations affecting positions for which no pathogenic substitution has been described in other serpins, mutants F214S, F281C, and M303T replace internally located hydrophobic residues with polar ones. Moreover, the F281C mutation introduces a free cysteine that may interfere with the normal disulfide-bond formation connecting C101 to C406 and C108 to C183 (Bock et al. 1986). However, the T372P substitution affects a residue not conserved in serpins (fig. 3*B*), and expression of this mutation in transfected cells should

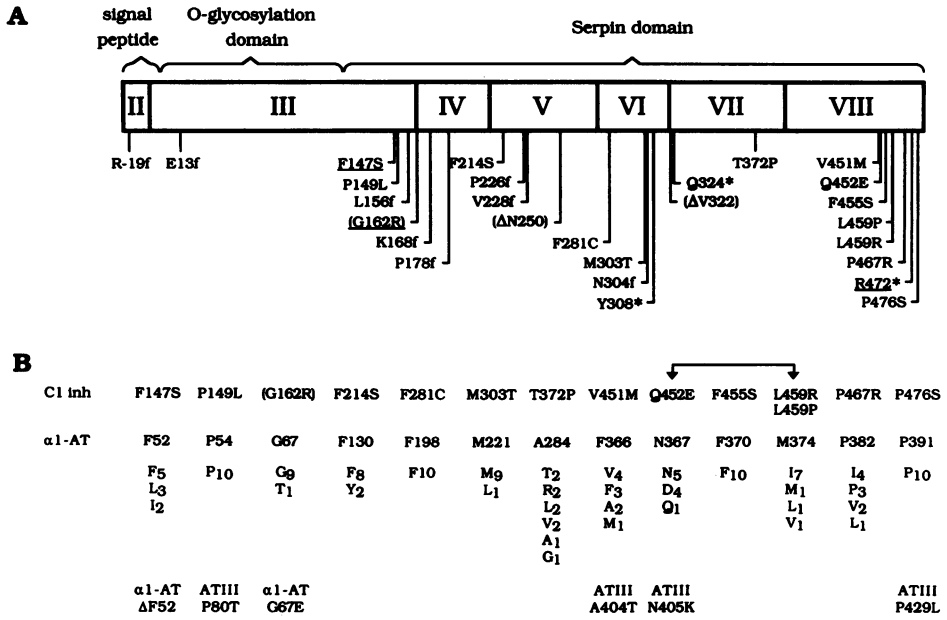

Figure 3 Mutations in the coding regions. *A*, Distribution of the mutations within the translated regions. The protein domains are indicated above the coding portion of the C1 inh mRNA, and roman numbers denote exons. Frameshift mutations are indicated with the last correct amino acid followed by the letter f, and nonsense mutations are marked with an asterisk. Mutations found twice, in unrelated patients, are underlined. Three mutants (indicated in parentheses) may not be expressed significantly at the protein level, because of possible additional pretranslational defects. *B*, Amino acid substitutions in mutant C1 inh proteins. For each C1 inh mutation, the corresponding amino acid of α1-antitrypsin (α1-AT) is shown, and, below the α1-AT line, the identity of amino acid residues is indicated at equivalent positions for 10 human "inhibitory" serpins (C1 inh, α1-antitrypsin, heparin cofactor II, antithrombin III, endothelial plasminogen activator inhibitor, placental plasminogen activator inhibitor, α1-antichymotrypsin, α2-antiplasmin, protein C inhibitor, and protease nexin-1). The connected arrows point to two substitutions found on the same allele. Antitrypsin (α1-AT) and antithrombin (AT III) substitutions or deletions indicated at the bottom of the figure correspond to α1-AT M_{malton} (ΔF52), $M_{mineral\ springs}$ (G67E), ATIII Oslo or Paris 3 (A404T), La Rochelle (N405K), and Budapest (P429L); for recent reviews, see the work of Stein and Carrell (1995) and Perry and Carrell (1996).

provide clues to its phenotypic consequences. The effects of substitutions in the carboxy-terminal portion of C1 inh (encoded in exon 8) have been studied by in vitro mutagenesis and cell transfection, and in each case intracellular transport and secretion were severely affected (Verpy et al. 1995). However, the mutant proteins V451M, P476S, and F455S are partially secreted but dysfunctional (Eldering et al. 1995). Patient 34 (F455S) also has a C→G transversion 320 nucleotides upstream from the transcription start site; however, this mutation was also found in a healthy brother (authors' unpublished data).

Double Mutations in cis

Double mutations in a *cis* configuration were found in patients 40, 25, and 31 (table 1). Patient 40 carries an allele with a double de novo point mutation. In cultured cells, expression of each mutation separately demonstrated that the Q452E change has little or no effect on C1 inh protein structure or function, whereas secretion of the L459P mutant is totally abolished (Verpy et al. 1995).

In addition to the F147S missense mutation, which affects a conserved amino acid residue, patient 25 has a T→C transition at position 566. Both this mutation and that giving rise to the F147S substitution were found in the proband's affected son, indicating that they reside on the same allele. However, position 566 is the second nucleotide of exon 2 and thus is not part of a consensus acceptor splice site. Moreover, it affects 5′ untranslated mRNA sequences remote from the translation initiation, and therefore this change probably has no effect on the transcript or the protein. The same mutation was found in patient 10, together with the pathogenic V451M change that results in strongly reduced secretion. For want of other family members, we were unable to determine whether this T→C transition is on the same chromosome of patient 10 as is the missense mutation V451M.

A promoter mutation (C→G transversion at position −40) and a 3-bp deletion in exon 5, predicting the deletion of residue N250 (α1-AT position 167), were found in patient 31 and cosegregate in his family (not shown). The promoter mutation affects a pyrimidine-rich region (−48 to −17; see fig. 4*C*) of potential H-DNA structure, containing a sequence element (−35 to −17) similar to

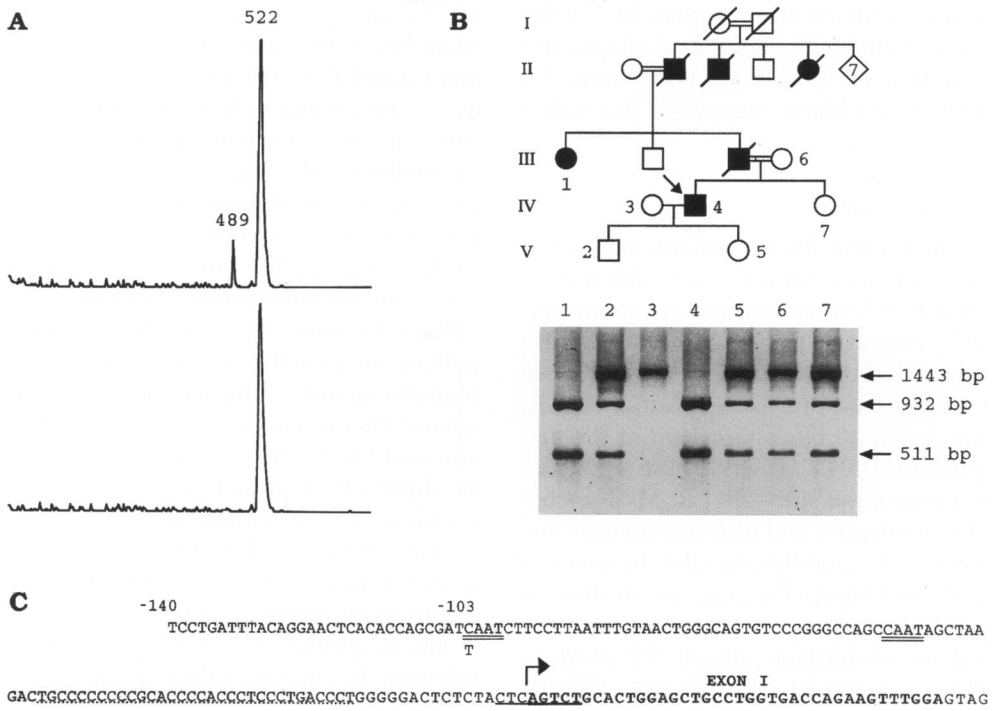

Figure 4 Detection of the homozygous promoter mutation −103 C→T. *A*, Detection of the mutation in the 522-bp-long fragment A1 by FAMA. The genomic DNA of patient 44 was mixed with an equal amount of control genomic DNA before the first amplification step. The profiles of the coding strands obtained on hydroxylamine modification (C specific) are shown for patient 44 (*upper profile*) and for another patient (unmutated amplicon; *lower profile*). Cleavage at the mismatched C in patient 44 generates a 489-nucleotide fragment. *B*, Status of family members with regard to the promoter mutation. Numbers next to symbols in the pedigree refer to lanes on the gel shown below it. The 1,443-bp-long fragment used in region A, obtained with the external primers (see table 1), was digested with *Ase*I (recognition sequence: ATTAAT). Note that, in addition to the proband IV 4 only patient III 1 is homozygous for the mutation. A preliminary clinical and biochemical characterization of this family has been published (La Rocca et al. 1986). *C*, Sequence of the relevant promoter region, with two potential CAAT boxes double-underlined. A pyrimidine-rich stretch with potential H-DNA structure (Davis et al. 1989) is underlined with dots, and an initiator sequence is underlined, encompassing the transcription start site, which is at an adenine residue (Carter et al. 1991; Zahedi et al. 1994).

a sequence found upstream of the human *c-myc* gene, which binds positive transcriptional regulators (Davis et al. 1989).

Homozygous Promoter Mutation

The FAMA procedure, in the heterozygous screening mode (i.e., free from external probes) applied here to a typically autosomal dominant disease, failed to detect mutations in only 3 of the 36 patients. Of these, only one (see below) had a family history of the disease, whereas the diagnosis of HAE was not formal, even on clinical accounts, in the two sporadic cases. Careful reexamination of complement parameters led to the detection of autoantibodies to C1 inh in one patient, who was therefore diagnosed as having a rare acquired form of angioedema (Jackson et al. 1986; Alsenz et al. 1987). It should be noted that this patient had originally been diagnosed as having type II HAE. The other uninformative patient, also a sporadic case, consistently had C1 inh levels at the lower limit of the normal distribution but had normal C4 levels. Thus, his pathology is not akin to HAE.

The PCR products of region A2 of the three patients who had failed to reveal mutations were sequenced directly, together with the PCR products of the five patients carrying mutations in this region. Quite unexpectedly, a mutation was found in the homozygous state in patient 44 (table 2 and fig. 4*C*). This C→T transition at position −103 alters the first nucleotide of a putative CAAT box and is homozygous because of consanguinity. Owing to the dominant mode of transmission of the disease, our strategy had been based on the assumption that pathogenic mutations would obligatorily be heterozygous and thus reference DNA needed not to be added to the test DNA. FAMA reassessment, performed throughout the seven *C1 INH* regions of this patient after addition of a reference DNA, readily identified this C→T transition (fig. 4*A*) in each of the overlapping regions A1 and A2 and ruled out mutations in exons or exon-intron boundaries. In addition to proband IV4,

only one other living family member (patient III 1 in fig. 4) has a severe form of HAE. This individual also carries the promoter mutation in the homozygous state. All other family members are heterozygous for this mutation (fig. 4*B*).

Genetic Markers in C1 INH

In addition to the known *Hgi*AI variants in exon 8 (G/A 16830), two new dimorphisms were detected in intron 4 and intron 6, when we screened for mutations in regions C and E, respectively (fig. 1). DNA sequence analysis demonstrated the transition G→A, 88 bases downstream of the last base of exon 4 (position 4573), and the transition A→G, 20 bases upstream of the first base of exon 7 (position 14011). Each of these mutations results in loss of a restriction site—that is, *Mnl*I (recognition site GAGG) in intron 4 and *Nsi*I (recognition site ATGCAT) in intron 6. To establish the allele frequencies for the *Mnl*I, *Nsi*I, and *Hgi*AI variants, we studied 50 unrelated Caucasian individuals. The following allele frequencies could be established: .69/.31 for $MnlI^{+/-}$, .28/.72 for $NsiI^{+/-}$, and .69/.31 for $HgiAI^{+/-}$. The frequencies for the *Hgi*AI variant are not different from those reported (.68/.32) in a sample of 17 individuals (Bock et al. 1986). Moreover, for the *Mnl*I and *Hgi*AI polymorphisms, the distribution of the + alleles (nucleotides G4573 and G16830, respectively) and the − alleles (nucleotides A4573 and A16830, respectively) was found to be concordant in each of the 50 individuals examined. This observation, duplicated by the identity of the allele frequencies of the *Hgi*AI and *Mnl*I polymorphisms, suggests the presence, at least in the Caucasian population, of two ancient haplotypes, one featuring the association of G4573 with G16830 and the other one associating A4573 with A16830.

Discussion

Simultaneous labeling of wild-type and mutant PCR fragments with strand-specific fluorescent dyes followed by chemical cleavage of mismatches (CCM) allows efficient detection of mutations in large DNA regions. Each single nucleotide substitution gives rise to at least two detectable cleavage products, and computer-aided analysis allows unambiguous detection of even weak cleavage signals, which typically have gone undetected by radiolabeling. The mutation is precisely localized, and the nature of the change often can be inferred from the specificities of the cleaving reagents and the direct recognition of the strand undergoing cleavage. Moreover, small insertions/deletions and replacements of more than one nucleotide all can be detected. Microdeletions or microinsertions of one or a few nucleotides yield at least one strong cleavage signal (see the example in fig. 5). Moreover, the destabilizing effect of unpaired bases favors the reactivity of adjacent positions (Cotton and Campbell 1989). Once a mutation is detected, limited sequencing of only one strand has invariably proved sufficient for confirmation, because position and kind of mutation are essentially known. Furthermore, the precision of localization is enhanced, even compared with the most favorable conditions of conventional CCM—that is, the use of radioactively end-labeled sense and antisense probes (Grompe et al. 1989; Cotton 1993)—because the weak but reproducible cleavage pattern on paired cytosine or thymine bases provides sequence-quality information. In many cases the sequence change could be diagnosed without sequencing and could be verified promptly by restriction-endonuclease digestion. New mutations were always distinguished readily—that is, without sequencing—from those previously known, and pathogenic mutations were easily detected amid harmless polymorphisms, present in three of the seven regions scanned (fig. 1).

The properties of enzymes, such as bacteriophage resolvases, in cleaving DNA mismatches (Mashal et al. 1995; Youil et al. 1995) may be conveniently incorporated into an enzymatic mode of FAMA to ensure even more rapid detection of mutations. However, FAMA in the configuration reported herein is so far the only mutation scanning method allowing 100% detection and precise positioning of the nucleotide change. Moreover, the wide scanning window of FAMA and its high sensitivity of detection of mutant amplicons in the presence of an excess of wild-type sequences (Verpy et al. 1994) make it ideally suited for mutation scanning at the mRNA level. When mutations are carried by rare or unstable mutant mRNAs—and thus, for practical purposes, are likely to be invisible to direct sequencing—precise positioning of the change(s) within large RT-PCR products—presently up to 1.4 kb (authors' unpublished data)—allows straightforward genomic targeting of the relevant exon(s), rather than requiring the sequencing of large numbers of clones representing the relevant RT-PCR product.

FAMA of the seven amplicons shown in figure 1 results in effective scanning of ~4 kb of DNA. Complete screening of the patients examined in this study, using both the hydroxylamine and the osmium tetroxide–modification reactions, requires ~12 runs of the Perkin Elmer/ABD DNA sequencer, with the 36-well format. Other mutation-scanning methods (reviewed in Cotton 1993; Grompe 1993)—in particular, SSCP and heteroduplex analysis and their variants—are commonly used in situations in which small amplicons are scanned for rapid detection of a varying fraction of mutations. Denaturing gradient-gel electrophoresis affords more reliable detection, but its scanning window is likewise not larger than ~500 bp, and extensive optimizations are required

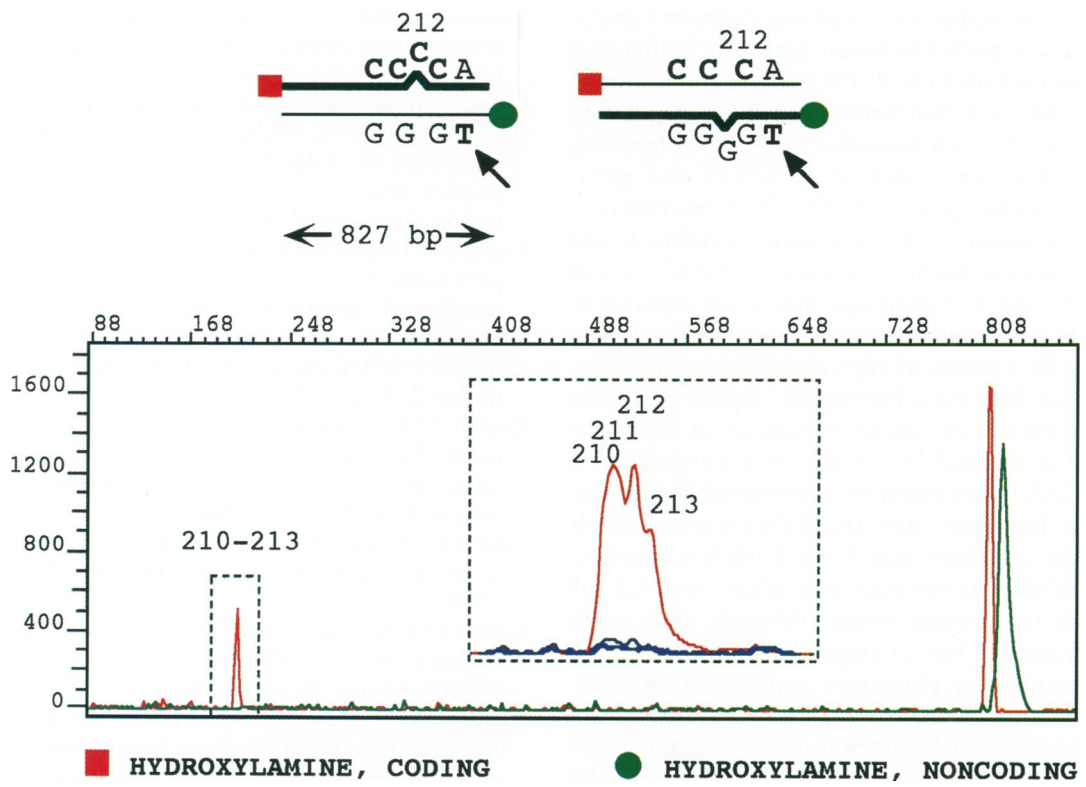

Figure 5 Example of microdeletion (for examples of point mutations, see Verpy et al. 1994). Whereas most mismatches are immediately visualized as new DNA fragments on the gel image, close examination of fluorometric tracings gives additional fine-structure information. In this example (microdeletion 8383 ΔC in exon 5), only one of the four possible unpaired C residues is represented schematically, and only the cleavage profiles (coding and noncoding strand) obtained on modification with hydroxylamine are shown. Note that microdeletions usually occur within short repeats, yielding rather broad cleavage peaks, as illustrated in the inset, in which the signal is expanded in both axes and compared with three control profiles from other individuals analyzed on the same gel. Furthermore, a thymidine residue at an adjacent position (*arrow*) yields a weak but distinct signal with osmium tetroxide, because of the destabilizing effect of unpaired bases (not shown).

for each locus to be scanned reliably. With each of these methods, extensive and good-quality DNA sequencing is necessary to identify the mutation(s). Estimates of the efficacy of detection of each method cannot be compared readily, because they vary, depending on the range of conditions tested, but it is generally believed that most of them are considerably below the 90% rate. Moreover, it is presently unknown whether particular types of nucleotide changes (e.g., microdeletions) are preferentially detected. Therefore, especially in the diagnostic setting, one should also consider the time and costs involved in the open-ended reexamination of false-negatives. In contrast, FAMA, in the robust protocol illustrated here, affords 100% mutation detection independently of sequence and involves the use of inexpensive reagents.

In our screening of HAE patients, heteroduplexes were produced directly after PCR on patient DNA—that is, without addition of wild-type DNA—since the disease is typically transmitted as an autosomal dominant trait. In three cases, no mutation was found on scanning all exons and ≥500 bp of the 5′ flanking region. On reexamination of the clinical and biological data, only patient 44 had typical type I HAE (i.e., quantitative C1 inhibitor deficiency), with several cases in the family. Instead, the initial diagnosis had been tentative for the other two patients, both sporadic cases. On the other hand, ≥7 of the 34 patients in whom *C1 INH* mutations were found had no family history of the disease, confirming our previous indications that de novo mutations occur frequently in HAE (Verpy et al. 1995; authors' unpublished data).

Direct sequencing of region A2 (fig. 1) of the *C1 INH* locus of patient 44 revealed a homozygous mutation affecting one of the two putative CAAT boxes (fig. 4). Homozygosity in this patient is clearly due to consanguinity (see the pedigree in fig. 4*B*). We have therefore repeated the FAMA scanning of all seven regions of the gene (fig. 1), using a strategy suited to the detection of homozygous mutations—that is, by mixing the genomic DNA of this patient with an equal amount of control genomic DNA. The −103 C→T substitution was confirmed by the cleavage products obtained in the overlapping fragments A1 and A2 (see an example in fig. 4*A*), but no other mutation was found within the *C1 INH* gene of this patient.

Relatively few naturally occurring promoter mutations have been reported in human genes, including fetal (gamma) globin (Ronchi et al. 1989; Sykes and Kaufman 1990), LDL receptor (Koivisto et al. 1994), coagulation factor IX (Crossley and Brownlee 1990; Crossley et al. 1992), retinoblastoma (Sakai et al. 1991), and gp91-phox genes (Newburger et al. 1994). The C→G transversion found at position −40 in patient 31 (table 2) and the C→T transition found in a putative CAAT box in patient 44 are the first promoter mutations reported in the *C1 INH* gene, and formal demonstration of their pathogenic effect awaits in vitro mutagenesis and transfection studies. However, barring the remote possibility of changes either in extragenic regions or in the intron sequences not scanned by FAMA, it is compelling to regard the CAAT-box mutation as responsible of pathogenic effects. The observation (fig. 4*B*) that in this family homozygosity correlates with low C1 inh levels and severe HAE, while heterozygous individuals have C1 inh levels within the normal range, although often at its lower limit, and are free of angioedema attacks, indeed reflects a quantitative phenotype expected from mutations in regulatory elements. Quantitative studies of the C1 inh mRNA obtained from monocytes of family members were hampered by lack of informativeness, in this family, of the *Hgi*AI site, the only polymorphism expressed at the mRNA level (fig. 1). Therefore, the functional consequences of this promoter mutation are being tested by in vitro mutagenesis and cell transfection.

In conclusion, the rapid and accurate mutation-scanning protocol illustrated here has proved very valuable for the diagnosis of HAE, a disease that is very heterogeneous at the molecular level, featuring a significant fraction of sporadic cases. Besides the vast diagnostic scope of the method, due to its robustness, its ability to detect all nucleotide changes allows one to sample rapidly the spectrum of mutations associated with a given disease, for the purpose either of establishing statistically informative and unambiguous genotype-phenotype correlations or eventually implicating alternative etiologies where, as often is the case, linkage studies are precluded.

Acknowledgments

M. Biasotto, who played a central role in the accomplishment of this work, died on July 17, 1995. This work was supported by grants from the Mutuelle Générale de l'Education Nationale and the Groupement de Recherches et d'Etudes sur les Génomes. During part of this work, E.V. was supported by a fellowship from the Pasteur-Weizmann Foundation.

References

Alsenz J, Bork K, Loos M (1987) Autoantibody-mediated acquired deficiency of C1 inhibitor. N Engl J Med 312:534–540

Biasotto M, Meo T, Tosi M, Verpy E (1996) FAMA: Fluorescence-assisted mismatch analysis by chemical cleavage. In: Landegren U (ed) Laboratory protocols for mutation detection. Oxford University Press, Oxford, pp 54–60

Bock SC, Skriver K, Nielsen E, Thøgersen H-C, Wiman B, Donaldson VH, Eddy RL, et al (1986) Human C1 inhibitor: primary structure, cDNA cloning, and chromosomal localization. Biochemistry 25:4292–4301

Carter PE, Duponchel C, Tosi M, Fothergill JE (1991) Complete nucleotide sequence for the C1 inhibitor with an unusually high density of *Alu* elements. Eur J Biochem 197: 301–308

Cotton R (1993) Current methods of mutation detection. Mutat Res 285:125–144

Cotton RGH, Campbell RD (1989) Chemical reactivity of matched cytosine and thymine bases near mismatched and unmatched bases in a heteroduplex between DNA strands with multiple differences. Nucleic Acids Res 17:4223–4229

Coutinho M, Aulak KS, Davis AE III (1994) Functional analysis of the serpin domain of C1 inhibitor. J Immunol 153: 3648–3654

Crossley M, Brownlee GG (1990) Disruption of a C/EBP binding site in the factor IX promoter is associated with haemophilia B. Nature 345:444–446

Crossley M, Ludwig M, Stowell KM, De Vos P, Olek K, Brownlee GG (1992) Recovery from hemophilia B Leyden: an androgen-responsive element in the factor IX promoter. Science 257:377–379

Curiel DT, Vogelmeier C, Hubbard RC, Stier LE, Crystal RG (1990) Molecular basis of α1-antitrypsin deficiency and emphysema associated with the α1-antitrypsin $M_{mineral\ springs}$ allele. Mol Cell Biol 10:47–56

Davis AE III (1988) C1 inhibitor and hereditary angioneurotic edema. Annu Rev Immunol 6:595–628

Davis AE III, Aulak K, Parad RB, Stecklein HP, Eldering E, Hack CE, Kramer J, et al (1992) C1 inhibitor hinge region mutations produce dysfunction by different mechanisms. Nat Genet 1:354–358

Davis TL, Firulli AB, Kinniburgh AJ (1989) Ribonucleoprotein and protein factors bind to an H-DNA-forming c-*myc* DNA element: possible regulators of the c-*myc* gene. Proc Natl Acad Sci USA 86:9682–9686

Eldering E, Verpy E, Roem D, Meo T, Tosi M (1995) COOH-terminal substitutions in the serpin C1 inhibitor that cause loop overinsertion and subsequent multimerization. J Biol Chem 270:2579–2587

Frangi D, Cicardi M, Sica A, Colotta F, Agostoni A, Davis AE III (1991) Nonsense mutations affect C1 inhibitor messenger RNA levels in patients with type I hereditary angioneurotic edema. J Clin Invest 88:755–759

Graham A, Kalsheker NA, Newton CR, Bamforth FJ, Powell SJ, Markham AF (1989) Molecular characterisation of three alpha-1-antitrypsin deficiency variants: proteinase inhibitor (Pi) $null_{cardiff}$ (Asp^{256}→Val); Pi M_{malton} (Phe^{51}→deletion) and Pi I (Arg^{39}→Cys). Hum Genet 84:55–58

Grompe M (1993) The rapid detection of unknown mutations in nucleic acids. Nat Genet 5:11–117

Grompe M, Muzny DM, Caskey CT (1989) Scanning detection of mutations in human ornithine transcarbamoylase by

chemical mismatch cleavage. Proc Natl Acad Sci USA 86: 5888–5892

Haris II, Green PM, Bentley DR, Giannelli F (1994) Mutation detection by fluorescent chemical cleavage: application to hemophilia B. PCR Methods Appl 3:268–271

Jackson J, Sim RB, Whelan A, Feighery C (1986) An IgG autoantibody which inactivates C1 inhibitor. Nature 323: 722–724

Janson M, Larsson C, Werelius B, Jones C, Glaser T, Nakamura Y, Jones CP, et al (1991) Detailed physical map of human chromosomal region 11q12-13 shows high meiotic recombination rate around *MEN1* locus. Proc Natl Acad Sci USA 88:10609–10613

Koivisto U-M, Palvimo JJ, Jänne OA, Kontula K (1994) A single-base substitution in the proximal Sp1 site of the human low density lipoprotein receptor promoter as a cause of heterozygous familial hypercholesterolemia. Proc Natl Acad Sci USA 91:10526–10530

Kwok P-Y, Carlson C, Yager TD, Ankener W, Nickerson DA (1994) Comparative analysis of human DNA variations by fluorescent-based sequencing of PCR products. Genomics 23:138–144

Lane DA, Olds RJ, Conard J, Boisclair M, Bock SC, Hultin M, Abildgaard U, et al (1992) Pleiotropic effects of antithrombin strand 1C substitution mutations. J Clin Invest 90:2422–2433

La Rocca E, Amoroso S, Brai M, Di Leonardo S, Aricò M (1986) Angioedema ereditario: indagini genealogiche e considerazioni cliniche sulle due forme genetiche in una casistica di 10 pazienti. G Ital Dermatol Venerol 121:203–208

Mashal RD, Koontz J, Sklar J (1995) Detection of mutations by cleavage of DNA duplexes with bacteriophage resolvases. Nat Genet 9:177–183

Millar DS (1995) Three novel missense mutations in the antithrombin III (AT3) gene causing recurrent venous thrombosis. Hum Genet 94:509–512

Newburger PE, Skalnik DG, Hopkins PJ, Eklund EA, Curnutte JT (1994) Mutations in the promoter region of the gene for gp91-*phox* in X-linked chronic granulomatous disease with decreased expression of cytochrome b 558. J Clin Invest 94: 1205–1211

Perry DJ, Carrell RW (1996) Molecular genetics of human antithrombin deficiency. Hum Mutat 7:7–22

Phelps RS, Chadwick RB, Conrad MP, Kronick MN, Kamb A (1995) Efficient, automatic detection of heterozygous bases during large-scale DNA sequence screening. Biotechniques 19:984–989

Ronchi A, Nicolis S, Santoro C, Ottolenghi S (1989) Increased Sp1 binding mediates erythroid specific overexpression of a mutated (HPFH) γ-globulin promoter. Nucleic Acids Res 17:10231–10241

Rosen FS, Charache P, Pensky J, Donaldson V (1965) Hereditary angioneurotic edema: two genetic variants. Science 148: 957–958

Rowley G, Saad S, Giannelli F, Green PM (1995) Ultrarapid mutation detection by multiplex, solid-phase chemical cleavage. Genomics 30:574–582

Sakai T, Ohtani N, McGee TL, Robbins PD, Dryja TP (1991) Oncogenic germ-line mutations in Sp1 and ATF sites in the human retinoblastoma gene. Nature 353:83–86

Senapathy P, Shapiro MB, Harris NL (1990) Splice junctions, branch point sites and exons: sequence statistics, identification and application to genome projects. Methods Enzymol 183:252–278

Siddique Z, McPhaden AR, Fothergill JE, Whaley K (1993) A point mutation in the C1-inhibitor gene causes type I hereditary angiooedema. Hum Hered 43:155–158

Siddique Z, McPhaden AR, Lappin DF, Whaley K (1991) An RNA splice site mutation in the C1-inhibitor gene causes type I hereditary angio-oedema. Hum Genet 88:231–232

Siddique Z, McPhaden AR, McCluskey D, Whaley K (1992) A single base deletion from the C1-inhibitor gene causes type I hereditary angio-oedema. Hum Hered 42:231–234

Stein PE, Carrell RW (1995) What do dysfunctional serpins tell us about molecular mobility and disease? Nat Struct Biol 2:96–113

Stoppa-Lyonnet D, Duponchel C, Meo T, Laurent J, Carter PE, Arala-Chaves M, Cohen JHM, et al (1991) Recombinational biases in the rearranged *C1-Inhibitor* genes of hereditary angioedema patients. Am J Hum Genet 49:1055–1062

Stoppa-Lyonnet D, Tosi M, Laurent J, Sobel A, Lagrue G, Meo T (1987) Altered C1-inhibitor genes in type I hereditary angioedema. N Engl J Med 317:1–6

Sykes K, Kaufman R (1990) A naturally occurring gamma globin gene mutation enhances SP1 binding activity. Mol Cell Biol 10:95–102

Verpy E, Biasotto M, Meo T, Tosi M (1994) Efficient detection of point mutations on color-coded strands of target DNA. Proc Natl Acad Sci USA 91:1873–1877

Verpy E, Couture-Tosi E, Eldering E, López-Trascasa M, Späth P, Meo T, Tosi M (1995) Crucial residues in the carboxy-terminal end of C1 inhibitor revealed by pathogenic mutants impaired in secretion or function. J Clin Invest 95:350–359

Youil R, Kemper BW, Cotton RGH (1995) Screening for mutations by enzyme mismatch cleavage with T4 endonuclease VII. Proc Natl Acad Sci USA 92:87–91

Zahedi K, Prada AE, Davis AE III (1994) Transcriptional regulation of the C1 inhibitor gene by γ-interferon. J Biol Chem 269:9669–9674